RECONSTRUCTING PLANAR CONVEX BODIES USING POINT X-RAYS FROM TWO SOURCES

JULIE LINMAN, OREGON STATE UNIVERSITY
JASON MURPHY, UNIVERSITY OF TEXAS AT AUSTIN

ADVISOR: DON SOLMON
OREGON STATE UNIVERSITY

ABSTRACT. This paper describes the implementation of an algorithm by Siefken and Spargo [8] to reconstruct convex bodies given discrete X-ray data from two point sources. We work with different initial approximations, compute both local and global error estimates, and attempt to show that for some fixed neighborhood N, we can approximate $\partial K \cap N$ arbitrarily close.

1 Introduction

Geometric Tomography is a subject that deals in part with retrieving information about convex bodies using X-rays. In particular, the problem of reconstruction is relevant in this field. Falconer [3] and Gardner [6] independently proved in 1983 that X-ray data from two points p and q uniquely determine a convex body K when the line l between them intersects the body's interior. In [3], Falconer states: "Production of a practical reconstruction algorithm and the error analysis, whilst feasible, would be complicated since this would involve the solution of non-linear simultaneous equations and equations defined by the limit of an iterative procedure." In 1991, Dartmann [2] developed an algorithm using X-ray data from two sources; he is the only person we know of to have implemented such an algorithm. In this paper, we implement a different algorithm of Siekfen and Spargo [8], developed in 2005, which also uses X-ray data from two sources. Specifically, we use discrete X-ray data to reconstruct the top halves of translated, rotated ellipses. We consider different initial approximations; explicitly compute base points following Falconer [3]; compute local error estimates; and work towards proving convergence on a fixed neighborhood of the base-points.

2 Definitions

Definition 2.1 *A **convex body**, K, is a compact, convex subset of the plane with non-empty interior. The boundary of K will be denoted ∂K.*

Definition 2.2 *A **source** is a point from which X-ray data is collected for a particular convex body. Without loss of generality, we assume that the sources are located on the line $\theta = 0$ in polar coordinates. Throughout this paper, the two sources, denoted p and q, will be located to the left and right of the convex body, respectively. The **base-line**, denoted l, is defined to be the line passing through p and q. Given a convex body K, the **base-points** are the points $l \cap \partial K$. The left and right base points will be labeled b_l and b_r, respectively.*

Definition 2.3 *Given a convex body K, a source p, and an angle $\phi \in [0, \pi)$, the **near-side point** is defined as the point in $l_\phi \cap \partial K$ that is the nearest to p, where l_ϕ is the line through p that makes an angle of ϕ with l, measured counterclockwise. The **far-side point** is defined as the point in $l_\phi \cap \partial K$ that is furthest from p. These definitions also hold for the source q.*

Definition 2.4 *The **near-side function** is defined as the distance from a source p to the near-side point on the body for each ϕ. The **far-side function** is defined as the distance from a source p to the far-side point on the body for each ϕ. The near-side and far-side functions for the source p will be denoted $r_p(\phi)$ and $R_p(\phi)$, respectively. Similarly, the near-side and far-side functions for the source q will be denoted $r_q(\psi)$ and $R_q(\psi)$, respectively.*

Definition 2.5 *Given a convex body K and a source p, the **point X-ray** of K at p is a function $X_{p,K}(\phi)$ (or $X_p(\phi)$ if no other bodies are being considered) defined on $[0,\pi)$, such that for all $\phi \in [0,\pi)$,*

$$X_p(\phi) = \lambda_l(K \cap l_\phi),$$

where l_ϕ is as defined above and λ_l signifies length. The point X-ray of K at p can equivalently be defined as $X_p(\phi) = R_p(\phi) - r_p(\phi)$. The point X-ray of K at q is defined similarly.

Definition 2.6 *The **supporting rays** for a convex body K from a source p are the rays emanating from p which intersect ∂K in either a point or a line segment. The **supporting angles** are the angles of inclination of the supporting rays.*

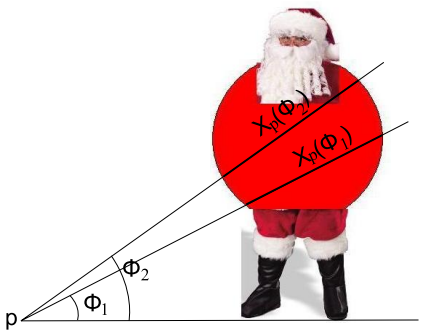

Figure 1: X-rays of a "Convex Body." $X_p(\phi)$ gives the length of intersection of the ray l_ϕ emanating from the base-line at angle ϕ with the body.

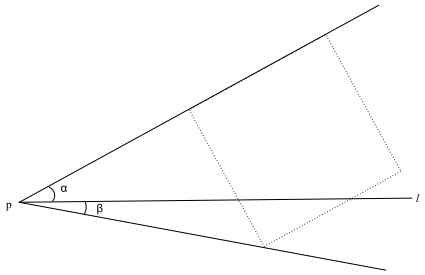

Figure 2: α and β are supporting angles for the body. l_α and l_β, the rays emanating from p at respective angles, are supporting rays for the body.

3 Pertinent Theorems and Description of the Algorithm

Definition 3.1 *A convex body K is said to be **determined** by X-ray functions at a set of points S if* $X_{s,K'}(\alpha) = X_{s,K}(\alpha)$ *for all* $s \in S$, $\alpha \in [0,\pi]$ *implies that* $K' = K$. *I.e. K is determined by X-ray functions at a set of points if the only convex body having these particular X-ray functions at these particular points is K itself.*

Falconer[4] and Gardner[6] proved independently that point X-rays from two sources uniquely determine a convex body K in certain instances. The statement of the following theorem comes from [7].

THEOREM *A convex body K is determined by X-rays at two points p and q in each of the following situations:*
(i) The line l through p and q meets int *K, p and q do not belong to* int *K, and the component of* $l \setminus (p,q)$ *intersecting K is specified;*
(ii) l supports K;
(iii) p, q belong to int *K.*

Throughout this paper, we consider case (i), specifically the case when our sources p and q lie on the left and right side of the body, respectively (as mentioned above). Knowing that X-ray data from two sources uniquely determine a body, one wonders if those same data can be used to efficiently reconstruct the body. Dartmann [2] came up with a reconstruction algorithm in 1991. His algorithm depends on the assumption of vertical tangent lines at the base-points; he uses a result of Falconer [3] (described below) to compute the base-points explicitly. He uses point-wise construction of a polygon to approximate a body K. During the Summer 2005 REU program in Mathematics at Oregon State University, Siefken and Spargo [8] developed a modified algorithm. It is this algorithm that we study.

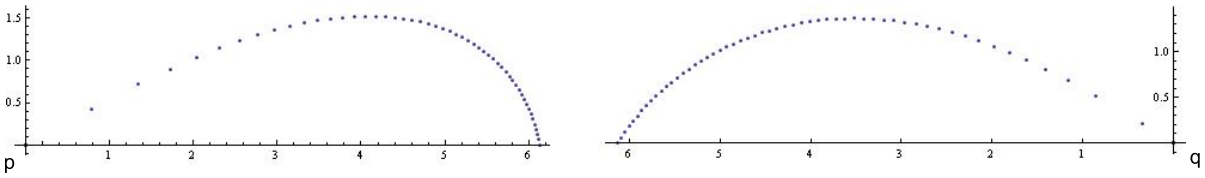

Figure 3: X-ray data for the upper half of ellipse #4 in Table 1, reconstructed in each of Sections 9.1, 9.2, and 9.3. Axes are centered at p and q, respectively.

3.1 Description of the Algorithm

Recall the functions $r_p(\phi)$, $R_p(\phi)$, $r_q(\psi)$, and $R_q(\psi)$, the near- and far-side functions of p and q, respectively. The values $r_p(0)$, $R_q(0)$, $r_q(0)$, and $R_q(0)$ come up frequently. $r_p(0)$ is the distance from p to b_l, $R_p(0)$ is the distance from p to b_r, $r_q(0)$ is the distance from q to b_r, and $R_q(0)$ is the distance from q to b_l.

In carrying out the algorithm, we use a discrete set of X-ray data from both sources, determined by some step size $\frac{\pi}{n}$ or equivalently by the number of X-rays n. Most often, in our cases $n = 314$. The algorithm requires first that one compute the base-points b_l and b_r. In Lemma 3 of [3], Falconer derives a formula which can be used to compute the base-points of a convex body using only the X-ray data from two sources.

LEMMA. *Let K be a convex body with X-ray functions $X_p(\phi)$ and $X_q(\psi)$ from sources p and q, where the line l between p and q cuts* int K. *We have:*

$$\lim_{\varepsilon\to 0}\left(\int_{\varepsilon}^{\pi-\varepsilon}\frac{X_q(\psi)}{\sin(\psi)}d\psi-\int_{\varepsilon}^{\pi-\varepsilon}\frac{X_p(\phi)}{\sin(\phi)}d\phi\right)=$$

$$2(R_p(0)\ln(R_p(0))-r_p(0)\ln(r_p(0))+r_q(0)\ln(r_q(0))-R_q(0)\ln(R_q(0))).$$

Restricting to measurements in polar coordinates centered at p, we write $m=X_p(0)=R_p(0)-r_p(0)$ and write B as the value of the integral. We then define

$$F(t)=t\ln|t|-(t-m)\ln|t-m|$$

and solve the non-linear system of equations

$$R_p(0)-r_q(0)=q-p$$

$$F(R_p(0))-F(r_q(0))=2B.$$

With $R_p(0)$ and $r_q(0)$ known, the base-points can be determined. We describe the process of approximating this integral in more detail in the next section.

Siefken and Spargo derive a formula for $r_p'(0)$ and suggest as an initial approximation a portion of the line tangent to ∂K at the base-line which passes through b_l. (In this paper, we also consider the cases in which the initial approximation is either a portion of a non-tangent line or a section of the osculating circle of the body at the baseline. See Sections 7.2 and 7.3 below.)

We call our initial approximation $\gamma_{p,1}$. Choosing some small angle ϕ_1, we add $X_p(\alpha)$ to the tangent line for each angle α in $[0,\phi_1]$ for which we have data. We define $\Gamma_{p,1}(\alpha):=\gamma_{p,1}(\alpha)+X_p(\alpha)$. Next, using the law of sines, we find the angle ψ_1 at which a ray emanating from q meets the point $\Gamma_{p,1}(\phi_1)$. We then change our coordinate system (again using the law of sines) to polar coordinates with q as the origin, and we call $\gamma_{q,1}(\psi)$ the same curve as $\Gamma_{p,1}(\phi)$, with angles now measured clockwise from q. (In carrying out the actual reconstruction, there is an issue that arises here: Since we have only a discrete set of X-ray data, we may not have X-ray values at the specific angles we need here. To get around this issue, we have Mathematica linearly interpolate $\Gamma_{p,1}$ before we define $\gamma_{q,1}$.)

We will similarly define $\Gamma_{q,1}(\beta):=\gamma_{q,1}(\beta)+X_q(\beta)$ for all β in $[0,\psi_1]$ for which we have data. We use the law of sines to find the angle ϕ_2 at which a ray emanating from p meets $\Gamma_{q,1}(\psi_1)$, switch back to polar coordinates with p as the origin, and say $\gamma_{p,2}(\phi)$ is the same curve as $\Gamma_{q,1}(\psi)$ (the same problem comes up again, so again we interpolate $\Gamma_{q,1}$ in Mathematica). Then proceeding as before, we add the X-ray data to $\gamma_{p,2}$ for all angles in $[0,\phi_2]$ (for which we have data) to come up wtih $\Gamma_{p,2}$. This process then continues. The sequence of angles (ϕ_k) is increasing. Once ϕ_k surpasses the supporting angle, the algorithm has finished. (In our reconstructions, this usually happens within a few iterations, where we call an iteration the process of constructing $\gamma_{p,k+1}$ from $\gamma_{p,k}$.)

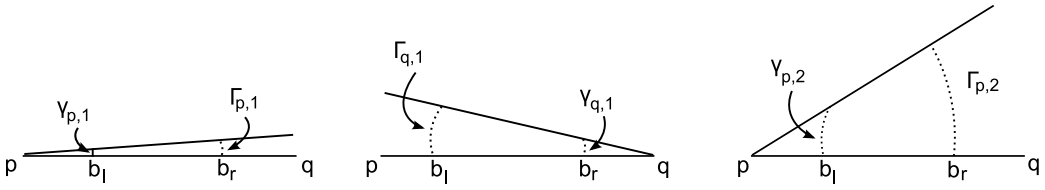

Figure 4: How the Algorithm Works

3.2 Implementation

Using Mathematica, we were able to implement the algorithm and reconstruct bodies from the class of rotated, translated ellipses. This choice was natural, since these are non-trivial bodies whose X-ray functions, derivatives, curvature, and base-points (i.e. all pertinent information) we can compute explicitly. These explicit computations provide us means of comparing our estimates to actual values. In the next section, we provide formulas related to translated, rotated ellipses. We discuss implementation and reconstruction in more detail below.

4 Ellipse Formulas

The equation for an ellipse is $\frac{x^2}{a^2}+\frac{y^2}{b^2}=1$. The equation for this same ellipse, now rotated θ radians and vertically translated $c \in \mathbb{R}$ is

$$x^2(b^2\cos^2(\theta)+a^2\sin^2(\theta))+x(y-c)(2b^2\cos(\theta)\sin(\theta)-2a^2\cos(\theta)\sin(\theta))+$$

$$(y-c)^2(b^2\sin^2(\theta)+a^2\cos^2(\theta))=a^2b^2.$$

We obtained an expression for the X-ray function of an ellipse with these parameters by computing the length of intersection of a ray emanating from a point p with the ellipse. The equation is:

$$X_p(\alpha)=2\sqrt{2}\sqrt{\frac{-(a^2b^2(-a^2-b^2+c^2+p^2+(c^2-p^2)\cos(2\alpha)+(a^2-b^2)\cos(2(\alpha-\theta))+2cp\sin(2\alpha)))}{(a^2+b^2+(-a^2+b^2)\cos(2(\alpha-\theta)))^2}}$$

when the expression under the radical is ≥ 0. We use the same function to get X-ray data for q.
We also computed the derivative and curvature for these ellipses, though we will not include them.
Since we know the base-points of our ellipse and the location of our sources, we are able to compute

$$2(R_p(0)\ln(R_p(0))-r_p(0)\ln(r_p(0))+r_q(0)\ln(r_q(0))-R_q(0)\ln(R_q(0))),$$

the exact value of Falconer's integral, which we approximate in order to locate the base-points.

Table 1: Ellipse specifications

Ellipse	a	b	θ	c	p	q
1	4	3	π/3	0	-5	6
2	4	3	7π/6	0	-5	6
3	4	3	0	-1	-5	6
4	4	3	π/3	-1	-5	6
5	4	3	π/3	0	5	6

5 Computing Base-Points

Recall Falconer's integral for computing base-points:

$$\lim_{\varepsilon\to 0}\left(\int_{\varepsilon}^{\pi-\varepsilon}\frac{X_q(\psi)}{\sin(\psi)}d\psi-\int_{\varepsilon}^{\pi-\varepsilon}\frac{X_p(\phi)}{\sin(\phi)}d\phi\right).$$

We begin with discrete X-ray data measured from angles increasing with a step size of $\Delta x=\frac{\pi}{n}$ for some n (most often 314, for us). We use this Δx and n to approximate the integral via the trapezoidal rule. We find

$$\left(\int_{\Delta x}^{\pi-\Delta x}\frac{X_q(\psi)}{\sin(\psi)}d\psi-\int_{\Delta x}^{\pi-\Delta x}\frac{X_p(\phi)}{\sin(\phi)}d\phi\right)\approx$$

$$\Delta x\left(\sum_{k=1}^{n-1}\frac{X_q(k\Delta x)}{\sin(k\Delta x)}-\frac{1}{2}(\frac{X_q(\Delta x)}{\sin(\Delta x)}+\frac{X_q((n-1)\Delta x)}{\sin((n-1)\Delta x)})\right)-\Delta x\left(\sum_{k=1}^{n-1}\frac{X_p(k\Delta x)}{\sin(k\Delta x)}-\frac{1}{2}(\frac{X_p(\Delta x)}{\sin(\Delta x)}+\frac{X_p((n-1)\Delta x)}{\sin((n-1)\Delta x)})\right).$$

In general, the error is O(Δx). If ∂K is C^2, then the error is O(Δx^2). This expression, involving only our discrete X-ray data, provides accurate calculations of the base-points, summarized in the following table:

Table 2: Error in Integral and Base-Point Computations, X-Ray data in steps of $\frac{\pi}{314}$

Ellipse	Computed Value of Integral	Actual Value of Integral	Computed Base-Points	Actual Base-Points
1	-2.65208	-2.65226	-3.17884, 3.17891	-3.17888, 3.17888
2	-3.2315	-3.2343	-3.65954, 3.66039	-3.65997, 3.65997
3	-3.38925	-3.38666	-3.77161, 3.77086	-3.77124, 3.77124
4	-1.44771	-1.448	-2.85254, 3.27807	-2.8526, 3.27802
5	-2.65208	-2.65226	-3.17916, 3.1786	-3.17888, 3.17888

6 Angle Approximations

For convenience, let $\Omega=\frac{R_p(0)R_q(0)}{r_p(0)r_q(0)}$ and $\Omega^{-1}=\frac{r_p(0)r_q(0)}{R_p(0)R_q(0)}$. Note that $\Omega>1$.

The reconstruction algorithm generates a sequence of iterates that approximate the convex body K. At the same time, however, the algorithm generates two sequences of angles. We begin with some small ϕ_1, the angle of inclination of the ray emanating from p that intersects some curve passing through b_l, the left base-point of our body K. This point of intersection is a point on our first iterate, namely $\gamma_{p,1}(\phi_1)$.

Another point on our first iterate is $\gamma_{p,1}(\phi_1)+X_p(\phi_1)=\Gamma_{p,1}(\phi_1)$. The algorithm proceeds by finding ψ_1, the angle of inclination of the ray emanating from q that intersects $\Gamma_{p,1}(\phi_1)$. We call this point of intersection $\gamma_{q,1}(\psi_1)$. Then repeating the process, we need to find ϕ_2, the angle of inclination of the ray emanating from p which intersects $\Gamma_{q,1}(\psi_1)=\gamma_{q,1}(\psi_1)+X_q(\psi_1)$. Two sequences are generated this way, namely $(\phi_k)_{k=1}^{\infty}$ and $(\psi_k)_{k=1}^{\infty}$. In general, we only have to worry about these angles until they grow larger than the supporting angle, which normally takes only a few iterations. Having estimates for these angles is useful in computing other error estimates related to the algorithm. This section describes the process by which we estimate these angles.

Before deriving the estimates, we make a few notes:

1. Each ψ_k is a function of ϕ_k, and each ϕ_{k+1} is a function of ψ_k.
2. It is clear that $\psi_k(0)=0$ and $\phi_k(0)=0$ for any k.
3. When we refer to arbitrary ϕ_k or ψ_k or refer to the angles as functions, we drop the subscript k.
4. From Siefken and Spargo[8], we have that $\psi'(0)=\frac{R_p(0)}{r_q(0)}$ and $\phi'(0)=\frac{R_q(0)}{r_p(0)}$.

Consider the Taylor expansion of $\psi(\phi)$ centered at ϕ=0, an accurate estimate for small angles.

$$\psi(\phi)=\psi(0)+\psi'(0)\phi+O(\phi^2)=0+\frac{R_p(0)}{r_q(0)}\phi+O(\phi^2).$$

So $\psi_k(\phi_k)\approx\frac{R_p(0)}{r_q(0)}\phi_k$.

Similarly, considering the Taylor expansion of $\phi(\psi)$ centered at 0 gives:

$$\phi(\psi)=\phi(0)+\phi'(0)\psi+O(\psi^2)=0+\frac{R_q(0)}{r_p(0)}\psi+O(\psi^2).$$

So $\phi_{k+1}(\psi_k)\approx\frac{Rq(0)}{rp(0)}\psi_k\approx\frac{R_p(0)R_q(0)}{r_p(0)r_q(0)}\phi_k=\Omega\phi_k$. Iterating this process, we find:

$$\phi_k\approx\Omega^{k-1}\phi_1 \tag{1}$$

and

$$\psi_k\approx\left(\frac{R_p(0)}{r_q(0)}\right)\Omega^{k-1}\phi_1. \tag{2}$$

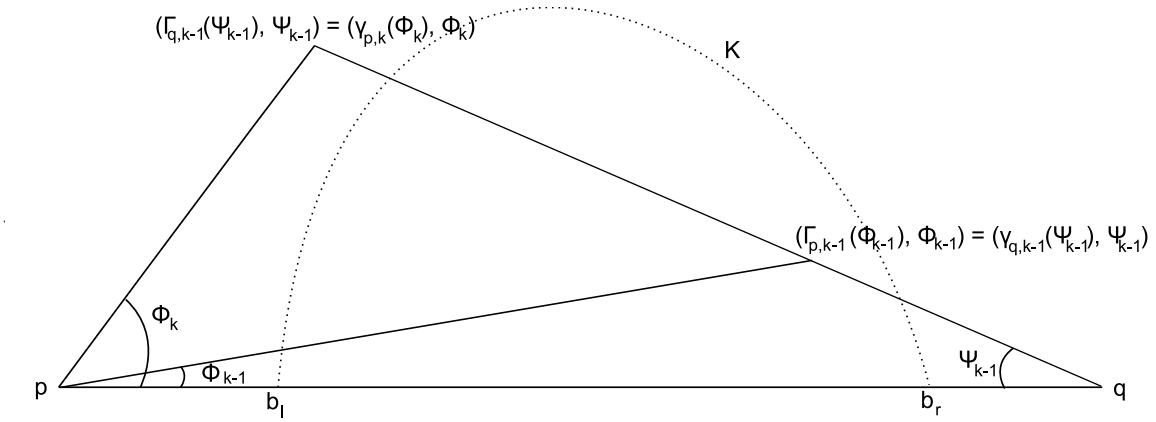

Figure 5: The sequence of angles being generated by the algorithm

7 Choices for Initial Approximation

In this section we describe three choices for the initial approximation $\gamma_{p,1}$.

7.1 Tangent Line

In [8], Siefken and Spargo suggest as their initial approximation a line tangent to ∂K which passes through b_l. To this end, they find an expression for $r'_p(0)$, the polar derivative of the body at b_l. The result is

$$r'_p(0) = \frac{-r_p(0)(R_p(0)X'_b(0))}{R_p(0)R_q(0) - r_p(0)r_q(0)}. \tag{3}$$

We use this polar derivative ($\frac{dr}{d\theta}$) to find the slope of the tangent line ($\frac{dy}{dx}$) to the curve $r_p(\theta)$. We write $r_p(\theta) = r$. Since $y = r\sin(\theta)$ and $x = r\cos(\theta)$, we get

$$\frac{dy}{d\theta} = \frac{dr}{d\theta}\sin(\theta) + r\cos(\theta)$$

and

$$\frac{dx}{d\theta} = \frac{dr}{d\theta}\cos(\theta) - r\sin(\theta),$$

so that

$$\frac{dy}{dx} = \frac{\frac{dy}{d\theta}}{\frac{dx}{d\theta}} = \frac{\frac{dr}{d\theta}\sin\theta + r\cos(\theta)}{\frac{dr}{d\theta}\cos(\theta) - r\sin(\theta)}.$$

Evaluating at $\theta = 0$, we get

$$\frac{dy}{dx} = \frac{r_p(0)}{r'_p(0)}. \tag{4}$$

We can now write an expression for the tangent line in polar coordinates centered at p. Let $f(\phi)$ denote the tangent line. Take $\alpha = \arctan(\frac{r_p(0)}{r'_p(0)})$ and consider the triangle $\triangle pb_lz$, where z is the point of intersection of the tangent line and the ray emanating from p at angle ϕ with the base-line l. The distance from p to z is $f(\phi)$.

The law of sines gives

$$\frac{r_p(0)}{\sin(\alpha-\phi)} = \frac{f(\phi)}{\sin(\alpha)},$$

so that

$$f(\phi) = \frac{r_p(0)\sin(\alpha)}{\sin(\alpha-\phi)}.$$

We now choose a small angle ϕ_1 and call our initial approximation $\gamma_{p,1}$ the section of $f(\phi)$ where ϕ is between 0 and ϕ_1.

Table 3: Error in Tangent Line Computations, X-Ray data in steps of $\frac{\pi}{314}$

Ellipse	Computed slope, left tangent	Actual slope, left tangent	Computed slope, right	Actual slope, right
1	4.70301	4.70128	4.7027	4.70128
2	3.54858	3.54658	3.54823	3.54658
3	2.12136	2.12132	-2.12118	-2.12132
4	2.25224	2.25199	-53.3953	-53.6598
5	4.70161	4.70128	4.69815	4.70128

7.2 Arbitrary Line Through Base-Point

It is possible to use an arbitrary line passing through b_l and carry out the reconstruction algorithm. While the tangent line is a better initial approximation, using a non-tangent line can help us understand how the algorithm works in general, similar to the idea of using noisy data.

The only difference in deriving the equation for this line in polar coordinates centered at p is that instead of letting $\alpha = \arctan(\frac{r_p(0)}{r_p'(0)})$, we simply let $\alpha = \arctan(m)$, where m is the slope of the line we want to use. If $g(\phi)$ is the equation for our arbitrary line, we find

$$g(\phi) = \frac{r_p(0)\sin(\alpha)}{\sin(\alpha-\phi)}.$$

We then choose our ϕ_1 and let $\gamma_{p,1}$ be the section of $g(\phi)$ where ϕ is between 0 and ϕ_1.

7.3 Osculating Circle at Base-Point

Definition 7.1 *The **curvature operator**,denoted $\mathcal{K}f$, characterizes the direction of concavity and is defined as*

$$\mathcal{K}f(\phi) = f(\phi)^2 + 2(f'(\phi))^2 - f(\phi)f''(\phi)$$

when f is C^2 at the angle ϕ. The curvature operator is positive (negative) when the graph of f at $(f(\phi),\phi)$ is concave toward (away from) the source.

Definition 7.2 *The **signed curvature** of a function f, denoted κ_f, is defined as*

$$\kappa_{f(\phi)} = \frac{f(\phi)^2 + 2(f'(\phi))^2 - f(\phi)f''(\phi)}{(f(\phi)^2 + (f'(\phi))^2)^{3/2}},$$

*when f is C^2 at the angle ϕ. Therefore, $\mathcal{K}f(\phi) = \kappa_{f(\phi)} \cdot (f(\phi)^2 + (f'(\phi))^2)^{3/2}$. The **curvature** of a function is the absolute value of its signed curvature.*

Definition 7.3 *The **osculating circle** of ∂K at b_l is the circle that has the same tangent, as well as the same curvature, as ∂K at b_l. The radius of the osculating circle is given by $\frac{1}{|\kappa_l|}$, where $|\kappa_l|$ is the curvature of ∂K at b_l.*

One can choose a section of the osculating circle of ∂K at b_l as an initial approximation for $\gamma_{p,1}$. In order to construct the osculating circle, we need to compute κ_l. Using the formula for the curvature operator of the sum of two functions given in Lemma 4.1 of [1], and recalling that $X_p(\phi) = R_p(\phi) - r_p(\phi)$, we have that

$$\mathcal{K}X_p(0) = \frac{X_p(0)}{R_p(0)}\mathcal{K}R_p(0) - \frac{X_p(0)}{r_p(0)}\mathcal{K}r_p(0) + 2r_p(0)R_p(0)\left(\frac{R_p'(0)}{R_p(0)} - \frac{r_p'(0)}{r_p(0)}\right)^2.$$

Let η and ω be the angles of inclination of the lines tangent to ∂K at b_l and b_r respectively (measured from the base-line l). Simple trigonometry then gives

$$\frac{R_p'(0)}{R_p(0)} - \frac{r_p'(0)}{r_p(0)} = \cot\omega - \cot\eta = \frac{\sin(\eta-\omega)}{\sin\eta\sin\omega}.$$

By definition,

$$\mathcal{K}R_p(0) := \kappa_r\left(R_p(0)^2 + R_p'(0)^2\right)^{3/2} = R_p(0)^3\kappa_r\left(1 + \left(\frac{R_p'(0)}{R_p(0)}\right)^2\right)^{3/2} = \frac{R_p(0)^3}{|\sin^3\omega|}\kappa_r.$$

Similarly,

$$\mathcal{K}r_p(0) := \kappa_l\left(r_p(0)^2 + r_p'(0)^2\right)^{3/2} = \frac{r_p(0)^3}{|\sin^3\eta|}\kappa_l.$$

Substituting this into the above equation and rearranging gives

$$\frac{R_p(0)^2}{|\sin^3\omega|}\kappa_r - \frac{r_p(0)^2}{|\sin^3\eta|}\kappa_l = \frac{\mathcal{K}X_p(0)}{X_p(0)} - 2\frac{r_p(0)R_p(0)}{X_p(0)}\frac{\sin^2(\eta-\omega)}{\sin^2\eta\sin^2\omega}. \tag{5}$$

A similar derivation from the source q gives

$$\frac{r_q(0)^2}{|\sin^3\omega|}\kappa_r - \frac{R_q(0)^2}{|\sin^3\eta|}\kappa_l = \frac{\mathcal{K}X_q(0)}{X_q(0)} - 2\frac{r_q(0)R_q(0)}{X_q(0)}\frac{\sin^2(\eta-\omega)}{\sin^2\eta\sin^2\omega}. \tag{6}$$

Note that

$$\frac{\mathcal{K}X_p(0)}{X_p(0)} = X_p(0) + 2\frac{X_p'(0)^2}{X_p(0)} - X_p''(0),$$

and that we have $\frac{\mathcal{K}X_q(0)}{X_q(0)}$ similarly.

Note the determinant of the coefficient matrix of the linear system (5) and (6) above is non-zero. We can then use Cramer's Rule to solve the system. Solving this system requires that we compute values of $X_p'(0)$, $X_q'(0)$, $X_p''(0)$, and $X_q''(0)$ from our discrete X-ray data. To this end, we use finite difference approximations. These computations provide accurate approximations for κ_l and κ_r without depending on K being convex. In fact, these computations determine the direction of the concavity of ∂K at the base-points. Results are summarized in the Table 4.

Table 4: Error in Signed Curvature Computations, X-Ray data in steps of $\frac{\pi}{314}$

Ellipse	Computed κ_l	Actual κ_l	Computed κ_r	Actual κ_r
1	-0.208778	-0.208753	0.208853	0.208753
2	-0.303628	-0.303552	0.303545	0.303552
3	-0.392444	-0.392483	0.392496	0.392483
4	-0.18996	-0.18994	0.248696	0.248674
5	-0.20874	-0.208753	0.208853	0.208753

After computing the curvature at b_l, we can construct the osculating circle of ∂K at b_l. The equation of a circle $r(\phi)$ with center (r_0, α) and radius R is given by

$$r(\phi)^2 - 2r(\phi)r_0\cos(\phi-\alpha) + r_0^2 = R^2.$$

The center of the osculating circle is found by adding a vector of magnitude $\frac{1}{|\kappa_l|}$ in the direction normal to ∂K at b_l. Call this point (c_0, β). Thus, the osculating circle of ∂K at b_l (in polar coordinates centered at p) is given by

$$r(\phi)^2 - 2r(\phi)c_0\cos(\phi-\beta) + c_0^2 = \left(\frac{1}{|\kappa_l|}\right)^2.$$

In some reconstructions, we choose a small angle ϕ_1 and let $\gamma_{p,1}$ be the section of the osculating circle between 0 and ϕ_1.

8 Local Error Estimates

In this section we derive error estimates for different initial approximations to the curve.

8.1 Tangent Line as Initial Approximation

Recall that $\Omega^{-1} = \frac{r_p(0)r_q(0)}{R_p(0)R_q(0)}$. Consider the case when the initial approximation is a line through b_l tangent to ∂K at b_l. Theorem 4.1 of Siefken and Spargo[8] gives an estimate for the local error on the ray emanating from source p at angle ϕ_k is given as:

$$E_{p,k}(\phi_k) = r_p(\phi_k) - \gamma_{p,k}(\phi_k) = -\Omega^{-2(k-1)}\frac{\kappa_l(r_p(0)^2 + r_p'(0)^2)^{3/2}}{r_p(0)}\phi_k^2 + O(\phi_k^3)$$

$$= -\Omega^{-2(k-1)} \frac{r_p(0)^2 \kappa_l}{|\sin^3 \eta|} \phi_k^2 + O(\phi_k^3),$$

where κ_l is the signed curvature of ∂K at b_l and the second form, which is more geometrically meaningful, comes from Section 7.3. Substituting in our angle approximation (1) for ϕ_k in the equation, one sees the term $\Omega^{-2(k-1)}$ will cancel out, and we are left with

$$E_{p,k}(\phi_k) \approx \frac{\kappa_l (r_p(0)^2 + r_p'(0)^2)^{3/2}}{r_p(0)} \phi_1^2 + O(\phi_k^3) = \frac{r_p(0)^2 \kappa_l}{|\sin^3 \eta|} \phi_1^2 + O(\phi_1^3).$$

8.2 Arbitrary Line Through Base-Point as Initial Approximation

Consider the case when the initial approximation is an arbitrary line passing through b_l. As usual, we call our approximations $\gamma_{p,k}(\phi)$. Let $E_{p,k}(\phi) = \gamma_{p,k}(\phi) - r_p(\phi)$ be the local error at angle ϕ in the kth iteration. Considering Taylor expansions of both $\gamma_{p,k}(\phi)$ and $r_p(\phi)$ centered at 0, we get:

$$E_{p,k}(\phi) = (\gamma_{p,k}(0) + \gamma_{p,k}'(0)\phi + O(\phi^2)) - (r_p(0) + r_p'(0)\phi + O(\phi^2))$$

$$= (\gamma_{p,k}'(0) - r_p'(0))\phi + O(\phi^2),$$

since $\gamma_{p,k}(0) = r_p(0)$. Here we are tacitly assuming ∂K is C^2 near base-points. (In general, we get the error is O(ϕ).)

The term we need to investigate, then, is $\gamma_{p,k}'(0) - r_p'(0)$. In [8], Siefken and Spargo derive an expression for $r_p'(0)$, so that we are left to find $\gamma_{p,k}'(0)$.

The law of sines with the triangle $\triangle pqx$, where x = $(\Gamma_{p,k}(\phi), \phi)$ = $(\gamma_{q,k}(\psi), \psi)$, gives

$$\frac{\gamma_{q,k}(\psi)}{\sin(\phi)} = \frac{\Gamma_{p,k}(\phi)}{\sin(\psi)}.$$

Following a very similar derivation from [8], we cross multiply and differentiate with respect to ϕ, considering ψ as a function of ϕ. We find

$$\psi'(\phi) = \frac{\Gamma_{p,k}'(\phi)\sin(\phi) + \Gamma_{p,k}(\phi)\cos(\phi)}{\gamma_{q,k}'(\psi)\sin(\psi) + \gamma_{q,k}(\psi)\cos(\psi)},$$

which, after substituting $\phi = 0$ (and so $\psi = 0$), gives $\psi'(0) = \frac{\Gamma_{p,k}(0)}{\gamma_{q,k}(0)} = \frac{R_p(0)}{r_q(0)}$.

Following still [8] we now consider the law of cosines on the same triangle to find

$$\gamma_{q,k}(\psi)^2 = (q-p)^2 + \Gamma_{p,k}(\phi)^2 - 2(q-p)\Gamma_{p,k}(\phi)\cos(\phi).$$

Differentiating with respect to ϕ, with ψ a function of ϕ, and solving for $\gamma_{q,k}'(\psi)$, we find that

$$\gamma_{q,k}'(\psi) = \frac{\Gamma_{p,k}(\phi)\Gamma_{p,k}'(\phi) - (q-p)\Gamma_{p,k}'(\phi)\cos(\phi) + (q-p)\Gamma_{p,k}(\phi)\sin(\phi)}{\gamma_{q,k}(\psi)\psi'(\phi)}.$$

We let ϕ (and therefore ψ) $= 0$ and substitute in our $\psi'(0)$, giving

$$\frac{\gamma'_{q,k}(0)}{r_q(0)} = \frac{-\Gamma'_{p,k}(0)}{R_p(0)}. \tag{7}$$

The same computations using the triangle $\triangle pqy$ where y = $(\gamma_{p,k}(\phi), \phi)$ = $(\Gamma_{q,k-1}(\psi), \psi)$ give

$$\phi'(0) = \frac{R_q(0)}{r_p(0)}$$

and

$$\frac{\gamma'_{p,k}(0)}{r_p(0)} = \frac{-\Gamma_{q,k-1}(0)}{R_q(0)}. \tag{8}$$

We now seek to find an expression for $\gamma'_{p,k}(0)$ in terms of $\gamma'_{p,1}(0)$. Recall $\Omega^{-1} = \frac{r_p(0)r_q(0)}{R_p(0)R_q(0)}$. We have,

$$\gamma'_{p,k}(0) = \frac{-r_p(0)}{R_q(0)}(\Gamma'_{q,k-1}(0)) = \frac{-r_p(0)}{R_q(0)}(\gamma'_{q,k-1}(0) + X'_q(0))$$

$$= \frac{-r_p(0)}{R_q(0)}\left(\frac{-r_q(0)}{R_p(0)}\Gamma'_{p,k-1}(0) + X'_q(0)\right) \text{ from (7)}$$

$$= \Omega^{-1}\left(\gamma'_{p,k-1}(0) + X'_p(0)\right) - \frac{r_p(0)}{R_q(0)}X'_q(0)$$

$$= \Omega^{-1}\gamma'_{p,k-1}(0) + \Omega^{-1}\left(R'_p(0) - r'_p(0)\right) - \frac{r_p(0)}{R_q(0)}\left(R'_q(0) - r'_q(0)\right).$$

From [8], we have $R'_q(0) = \frac{-R_q(0)}{r_p(0)}r'_p(0)$ and $r'_q(0) = \frac{-r_q(0)}{R_p(0)}R'_p(0)$. Substituting these equations into the last term, we get

$$\gamma'_{p,k}(0) = \Omega^{-1}\gamma'_{p,k-1}(0) + \Omega^{-1}(R'_p(0) - r'_p(0)) + r'_p(0) - \Omega^{-1}R'_p(0)$$
$$= \Omega^{-1}(\gamma'_{p,k-1}(0) - r'_p(0)) + r'_p(0).$$

We can now begin to iterate this process of substitution to work towards an expression for $\gamma'_{p,k}(0)$ in terms of $\gamma'_{p,1}(0)$. We will write $\gamma'_{p,k-1}(0)$ in terms of $\gamma'_{p,k-2}(0)$:

$$\gamma'_{p,k}(0) = \Omega^{-1}\left(\Omega^{-1}(\gamma'_{p,k-2}(0) - r'_p(0)) + r'_p(0) - r'_p(0)\right) + r'_p(0)$$

$$= \Omega^{-2}\left(\gamma'_{p,k-2}(0) - r'_p(0)\right) + r'_p(0).$$

Following this process, we see

$$\gamma'_{p,k}(0) = \Omega^{-(k-1)}(\gamma'_{p,1}(0) - r'_p(0)) + r'_p(0),$$

so that

$$\gamma'_{p,k}(0) - r'_p(0) = \Omega^{-(k-1)}\left(\gamma'_{p,1}(0) - r'_p(0)\right).$$

Inserting this equation into our expression for $E_{p,k}(\phi)$ and using our angle approximation from (1), we get

$$E_{p,k}(\phi_k) = (\Omega^{-(k-1)})(\gamma'_{p,1}(0) - r'_p(0)))\phi_k$$
$$\approx \Omega^{-(k-1)}(\gamma'_{p,1}(0) - r'_p(0))\Omega^{k-1}\phi_1$$
$$= (\gamma'_{p,1}(0) - r'_p(0))\phi_1 = E_{p,1}(\phi_1).$$

One note worth making is that our angle approximation works better for smaller angles. We see, then, that the local error measured at small angles stays approximately equal to the initial local error for the case of an arbitrary line for an initial approximation.

An alternate, geometrically informative expression for $E_{p,1}(\phi)$ is

$$r_p(0)\frac{\sin(\eta - \alpha)}{\sin\eta \sin\alpha}\phi,$$

where η is the angle of inclination of the line tangent to ∂K at b_l and α is the angle of inclination of $\gamma_{p,1}$, both measured counterclockwise from l. We arrive at this expression using a derivation similar to that in Section 7.3.

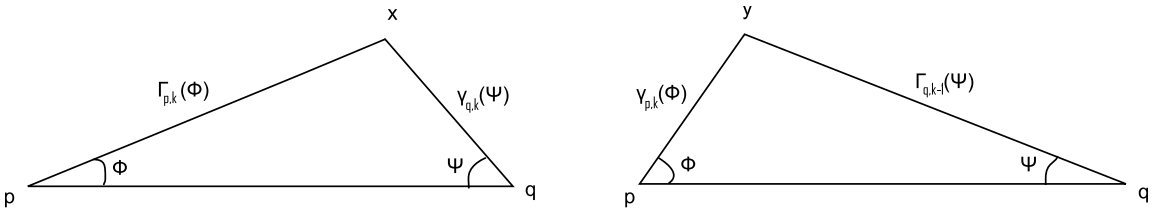

Figure 6: Triangles used in derivation of error estimate for non-tangent initial approximation

8.3 Osculating Circle at Base-Point as Initial Approximation

Using an osculating circle as an initial approximation gives us an initial local error $E_{p,1}(\phi_1)$ on the order of $(\phi_1)^3$ when ∂K is C^4. By considering Taylor expansions about 0, it is clear that

$$E_{p,1}(\phi_1) = r_p(\phi_1) - \gamma_{p,1}(\phi_1)$$
$$= (r_p(0) + r'_p(0)\phi_1 + r''_p(0)\phi_1^2 + r'''_p(0)\phi_1^3) - (\gamma_{p,1}(0) + \gamma'_{p,1}(0)\phi_1 + \gamma''_{p,1}(0)\phi_1^2 + \gamma'''_{p,1}(0)\phi_1^3) + O(\phi_1^4)$$
$$= (r'''_p(0) - \gamma'''_{p,1}(0))\phi_1^3 + O(\phi_1^4),$$

since the function value, first derivative, and second derivative of r_p and $\gamma_{p,1}$ are equal at 0.

We didn't carry out detailed computations for the osculating circle, because computations of the third derivatives of r_p would be extremely messy. Our main interest was to see how much better the reconstructions went with a better initial approximation; we found there not to be a significant difference between the tangent line case and the osculating circle case. (See Section 9 below.)

9 Reconstructions

We were able to implement the algorithm for translated, rotated ellipses using Mathematica. For all of the reconstructions here, we used a step size of $\frac{\pi}{314}$ for our X-ray data and an initial angle $\phi_1 = \frac{10\pi}{314}$ (i.e. we used 11 X-ray data points in the initial approximation, $\gamma_{p,1}$). Since the angles ϕ_k increase, and the algorithm stops once ϕ_k surpasses the supporting angle, we often see only a few iterates (generated from p) of the algorithm before it finishes. We show only iterates generated from p, and in each reconstruction image, we show in the background the ellipse being reconstructed.

9.1 Tangent Line as Initial Approximation

Using the segment of the tangent line of ∂K at b_l where $\phi \in [0, \phi_1]$ as our initial approximation, $\gamma_{p,1}$, we reconstructed the upper half of several different translated, rotated ellipses. (Reconstructing the lower half of these ellipses should follow the same algorithm.) We saw that after a few iterations of the algorithm, our reconstructions closely approximate ∂K. Below we show the first few iterates (generated from p) of our reconstructions of ellipses #2 and #4, specified in Table 1.

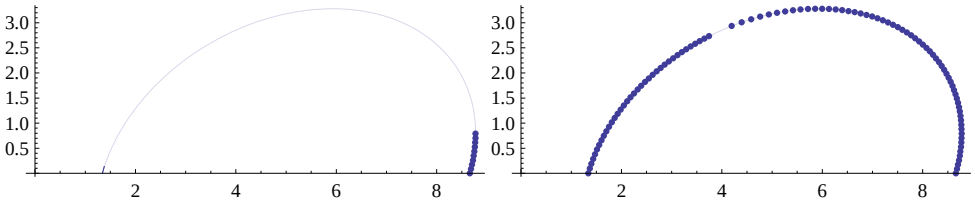

Figure 7: Reconstructing Ellipse #2 with Tangent Line Approximation

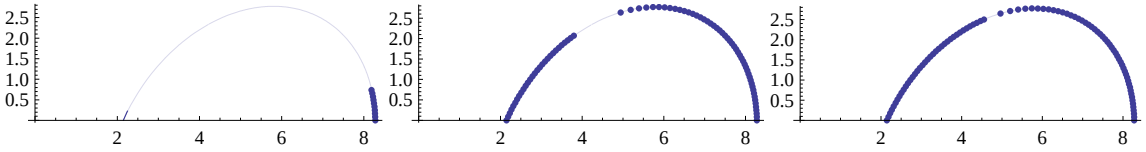

Figure 8: Reconstructing Ellipse #4 with Tangent Line Approximation

9.2 Arbitrary Line Through Base-Point as Initial Approximation

We also reconstructed several rotated, translated ellipses using an arbitrary line through b_l as $\gamma_{p,1}$. We varied the slope of this arbitrary line and found that even for (nonzero) slopes that are far from the slope of the tangent line of ∂K at b_l, the iterates of the algorithm appear to converge towards ∂K within a few iterations. Following are the first three iterates (generated from p) of our reconstruction of ellipse #4, where $\gamma_{p,1}$ is the line through b_l with slope 1.

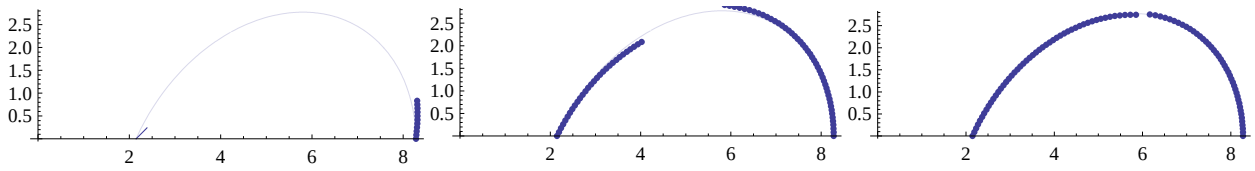

Figure 9: Reconstructing Ellipse #4 with Non-Tangent Line Approximation

9.3 Osculating Circle at Base-Point as Initial Approximation

Additionally, we reconstructed several rotated, translated ellipses using the portion of the osculating circle of ∂K at b_l where $\phi \in [0, \phi_1]$ as $\gamma_{p,1}$. We saw that after a few iterations of the algorithm, these reconstructions closely approximate ∂K. However, we did not see any significant difference between using a portion of the osculating circle (compared to a portion of the tangent line) as our initial approximation. Below are the first four iterates (generated from p) of our reconstruction of ellipse #4.

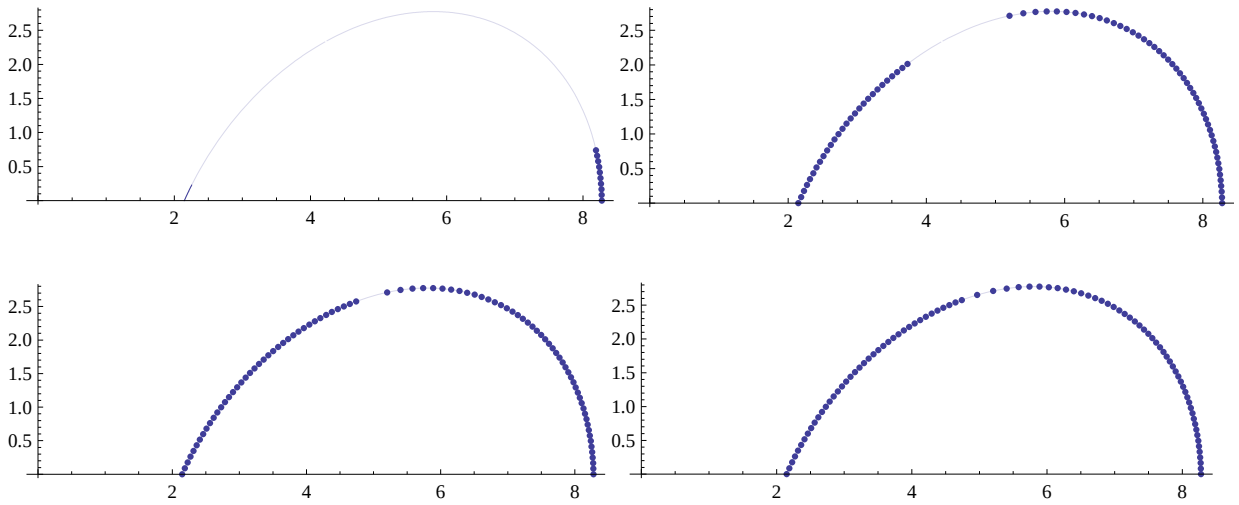

Figure 10: Reconstructing Ellipse #4 with Osculating Circle Approximation

10 Convergence on a Fixed Neighborhood

10.1 μ-error

Here we discuss what is called the μ-error, which seems to provide the best route towards proving convergence of the algorithm.

Definition 10.1 *The **characteristic function** of a set S, χ_S, is the function defined to be 1 on points in S and 0 otherwise.*

Definition 10.2 *The **μ-measure** of some area B is defined as*

$$\mu(B) = \int\int_{\mathbb{R}^2} \frac{\chi_B(x,y)}{|y|} dA.$$

The μ-measure can be shown to equal in polar form

$$\int_0^{2\pi}\int_0^{\infty}\frac{\chi_B(r,\theta)}{|\sin(\theta)|}drd\theta.$$

Definition 10.3 *Let K be a convex body between two sources p and q, where the line segment l between p and q intersects int K. Let f be a Lipschitz function approximating ∂K with the following properties:*

1. *f is defined on [0, α] for some α, with angles measured from l*
2. *$(f(0),0) = b_l$.*

*We define the **μ-error**, $E_\mu(f)$ to be $\mu(K_f)$, the μ-measure of the body formed by ∂K, the graph of f, and the ray l_α emanating from p with angle of inclination α.*

Note:

1. *Here we assume that the graph of f and ∂K do not cross on [0, α].*
2. $\int_0^{\infty}\frac{\chi_{K_f}(r,\theta)}{|\sin(\theta)|}dr = \frac{|r_p(\theta)-f(\theta)|}{\sin(\theta)}$, *if f approximates the near-side of ∂K w.r.t. p.*
3. *We can define μ-error similarly from q by using rays emanating from q.*

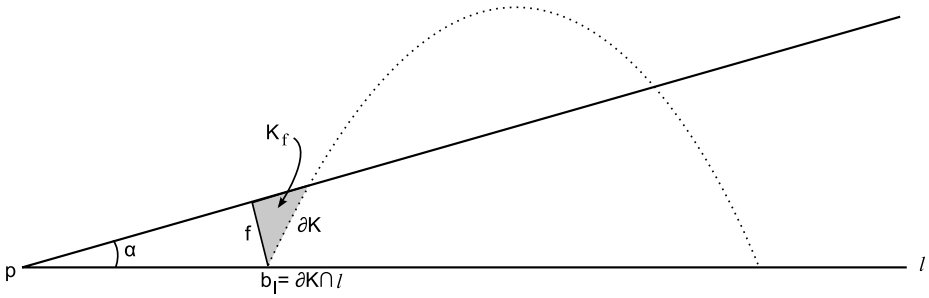

Figure 11: Picturing the body K_f. We say $E_\mu(f) = \mu(K_f)$.

The μ-error has some nice properties. For example, if γ and Γ are our first near- and far-side approximations (from p), defined up to the angle ϕ_1, we have the nice property that $E_\mu(\gamma) = E_\mu(\Gamma)$. Siefken and Spargo [8] show this explicitly. Since our notation is slightly different, we provide the computation here:

Lemma 10.4 $E_\mu(\gamma) = E_\mu(\Gamma)$

Proof:

$$E_\mu(\gamma) = \mu(K_\gamma) = \int_0^{2\pi}\int_0^{\infty}\frac{\chi_{K_\gamma}(r,\theta)}{|\sin(\theta)|}drd\theta = \int_0^{\phi_1}\int_0^{\infty}\frac{\chi_{K_\gamma}(r,\theta)}{\sin(\theta)}drd\theta$$

$$= \int_0^{\phi_1}\frac{r_p(\theta)-\gamma(\theta)}{\sin(\theta)}d\theta = \int_0^{\phi_1}\frac{X_p(\theta)+r_p(\theta)-X_p(\theta)-\gamma(\theta)}{\sin(\theta)}d\theta$$

$$= \int_0^{\phi_1}\frac{(X_p(\theta)+r_p(\theta))-(X_p(\theta)+\gamma(\theta))}{\sin(\theta)}d\theta = \int_0^{\phi_1}\frac{R_p(\theta)-\Gamma_p(\theta)}{\sin(\theta)}d\theta$$

$$= \int_0^{\phi_1}\int_0^{\infty}\frac{\chi_{K_\Gamma}(r,\theta)}{\sin(\theta)}drd\theta = \int_0^{2\pi}\int_0^{\infty}\frac{\chi_{K_\Gamma}(r,\theta)}{|\sin(\theta)|}drd\theta = \mu(K_\Gamma) = E_\mu(\Gamma).\surd$$

Another nice property of the μ-error is that it decreases as we iterate the algorithm. See Figure 13 in the Section 10.2 for a geometric presentation of this fact. Our angle approximations imply that the angles increase in general, but we do not have a positive lower bound for the rate of increase. We address this issue as well when discussing local convergence.

Our eventual goal is to prove that given a convex body K and an $\varepsilon > 0$, we can generate via the algorithm a body K' within ε of K in terms of μ-measure. First, we hope to show local convergence on a fixed neighborhood N of b_l, i.e. given $\varepsilon > 0$ we can generate via the algorithm an approximation within ε of $\delta K \cap N$ in terms of μ-measure.

10.2 Bounds on $E_\mu(\gamma_{p,n})$

Take $\gamma_{p,n}(\phi)$, our n^{th} approximation to ∂K. We have that $\gamma_{p,n}$ lies to the left of K. Let $f(\phi)$ be a Lipschitz function whose graph passes through b_l such that for some small angle α, we have $\phi \in (0,\alpha] \Rightarrow$

$$\gamma_{p,n}(\phi) < r_p(\phi) < f(\phi). \tag{9}$$

By construction, all three functions have the value $r_p(0)$ at $\phi = 0$.

Pick $\phi \in (0,\alpha)$. Consider the body T with vertices b_l, $(\gamma_{p,n}(\phi),\phi)$, and $(f(\phi),\phi)$. You can equivalently define T as the body consisting of sides
(1) $\gamma_{p,n}(\phi)$ for $\phi \in [0,\phi]$,
(2) $f(\phi)$ for $\phi \in [0,\phi]$, and
(3) the line segment connecting $(\gamma_{p,n}(\phi),\phi)$ and $(f(\phi),\phi)$.

The triangle of the right-hand side of Figure 14 gives an example of such a body, with f a line and $\gamma_{p,1}$ as the approximation in question.

Lemma 10.5 $E_\mu(\gamma_{p,n}) < \mu(T)$

Proof:
Beginning as in Lemma 10.4, we get

$$E_\mu(\gamma_{p,n}) = \int_0^\phi \frac{r_p(\theta)-\gamma_{p,n}(\theta)}{\sin(\theta)}d\theta < \int_0^\phi \frac{f(\theta)-\gamma_{p,n}(\theta)}{\sin(\theta)}d\theta, \quad \text{from (9)}$$

$$= \int_0^\phi \frac{f(\theta)-r_p(\theta)+r_p(\theta)-\gamma_{p,n}(\theta)}{\sin(\theta)}d\theta$$

$$= \int_0^\phi \frac{f(\theta)-r_p(\theta)}{\sin(\theta)}d\theta + \int_0^\phi \frac{r_p(\theta)-\gamma_{p,n}(\theta)}{\sin(\theta)}d\theta$$

$$= \int_0^\phi \int_0^\infty \frac{\chi_{K_f}(r,\theta)}{\sin(\theta)}drd\theta + \int_0^\phi \int_0^\infty \frac{\chi_{K_{\gamma_{p,n}}}(r,\theta)}{\sin(\theta)}drd\theta, \quad \text{from the definition of } \mu\text{-error}$$

$$= E_\mu(f) + E_\mu(\gamma_{p,n} = \mu(K_f) + \mu(K_{\gamma_{p,n}}) = \mu(K_f \cup K_{\gamma_{p,n}}), \quad \text{since } K_f \cap K_{\gamma_{p,n}} = \emptyset \text{ by construction}$$

$$= \mu(T), \quad \text{since } T = K_f \cup K_{\gamma_{p,n}} (\text{See Figure 12}). \surd$$

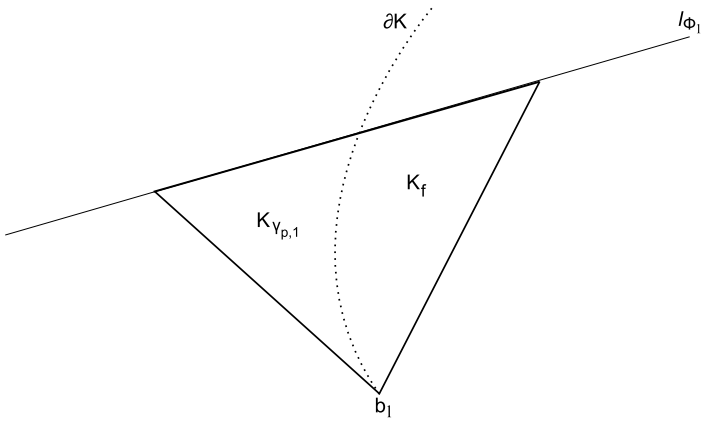

Figure 12: $T = K_f \bigcup K_{\gamma_{p,1}}$. In the lemma, we consider a more general case.

Denote the map described in our algorithm by σ. For example, we have that $\sigma(\gamma_{p,j}) = \gamma_{p,j+1}$. Denote by τ the conversion from polar coordinates centered at p to polar coordinates centered at q. It is clear that τ^{-1} converts from q-coordinates to p-coordinates. The map σ can be thought of essentially as the composition of the maps τ^{-1}, s_q, τ, and s_p, where $s_p(\gamma_{p,j}) = \Gamma_{p,j}$ and $s_q(\gamma_{q,j}) = \Gamma_{q,j}$. (In easier terms, s_p adds X-ray data from p, and s_q adds X-ray data from q.) More accurately $\sigma(f) = \tau^{-1}(s_q(\tau(s_p(f))))$ for a function f. We can also think of σ acting on individual points.

Given some $\varepsilon > 0$, suppose we take a body T_1 constructed as above s.t. $\mu(T_1) < \varepsilon$. We can then apply s_p to T_1 (see Figure 13). Analogous to the proof of Lemma 10.4 is the proof that $\mu(T_1) = \mu(s_p(T_1))$. When we take the ray from q that intersects the vertex of $s_p(T_1)$ inside K, we generate a new body T_2 and decrease the μ-measure. Again analogously we have that $\mu(T_2) = \mu(s_q(T_2))$. We define T_3 similar to how we defined T_2, i.e. we take the ray connecting p and the vertex of $s_q(T_2)$ inside of K. We see then that $\mu(T_3) < \mu(s_q(T_2) < \mu(T_1)$. If we continue this process, we see the following:

Lemma 10.6 *In the construction above, $\mu(T_{2n-1}) < \mu(T_1)$ for all T_{2n-1} we construct.*

Note 1: Notice that the angle of the ray connecting p and vertex of $s_q(T_{2k})$ will be less than the angle connecting p and $\gamma_{p,k}$ for all $k > 1$. This is worth keeping in mind and will be discussed later.

Note 2: If the angle between p and the vertex of $s_q(T_{2k})$ inside K is greater than the support angle of our body K for some k, the process stops. In many cases, this happens quickly. In general, however, we cannot assume this happens.

Note 3: As we generate a sequence of bodies, ∂K stays between our approximates and the curves generated by our initial line $f(\phi)$. This is fairly clear, since to get from T_1 to $s_p(T_1)$ we add X-ray data at each angle, which preserves the inequalities in (9), since $R_p(\phi) = r_p(\phi) + X_p(\phi)$. We find T_2 by measuring $s_p(T_1)$ from q up to a smaller angle; we do nothing to change the orientation of ∂K or the two sides of our body. As we repeat this process, ∂K should stay between the two sides of the bodies generated.

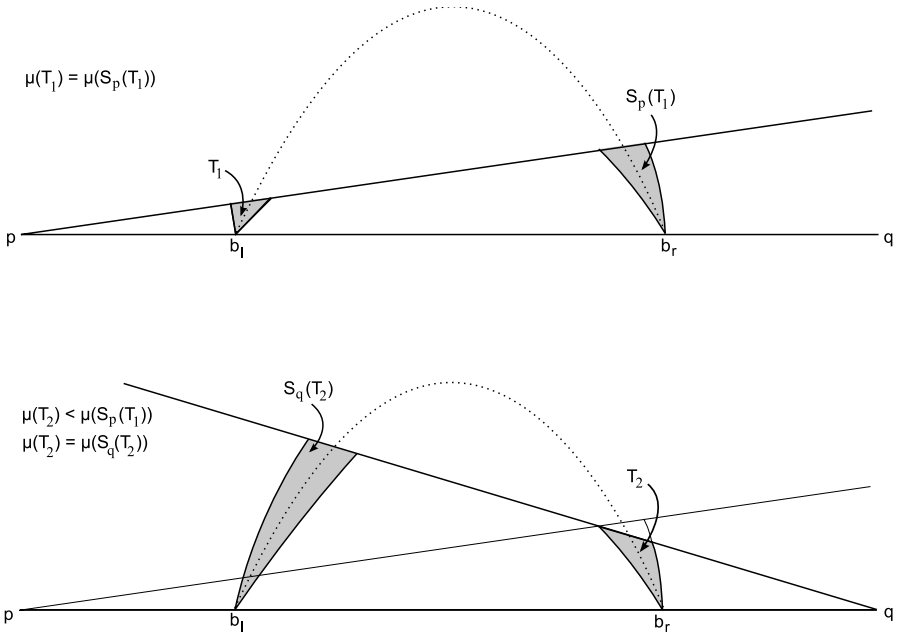

Figure 13: Geometric presentation of decreasing μ-error

10.3 Constructing T_1 with $\mu(T_1) < \varepsilon$

The bounds established above don't help us if we can't come up with some body T_1 with $\mu(T_1) < \varepsilon$. Fortunately, we can find such a body.

In [5], Fithian gives a formula for the μ-measure of a triangle. Specifically,

$$\mu(T) = l_0 \ln(1 + \frac{l_2}{l_1}) \tag{10}$$

where T is the triangle in Figure 14. Consider the triangle T_1 in the same figure, as described just before Lemma 10.5. Using Fithian's equation, we get

$$\mu(T_1) = r_p(0) \ln\left(1 + \frac{f(\phi) - \gamma_{p,1}(\phi)}{\gamma_{p,1}(\phi)}\right) = r_p(0) \ln\left(\frac{f(\phi)}{\gamma_{p,1}(\phi)}\right).$$

If we want $\mu(T_1) < \varepsilon$, then we need

$$\frac{f(\phi)}{\gamma_{p,1}(\phi)} < \exp\left(\frac{\varepsilon}{r_p(0)}\right).$$

Since $\varepsilon > 0$, we have $\exp(\frac{\varepsilon}{r_p(0)}) - 1 := \varepsilon^* > 0$. On the other hand, since $f(0) = \gamma_{p,1}(0) = r_p(0)$, we have that $\lim_{\phi \to 0} \frac{f(\phi)}{\gamma_{p,1}(\phi)} = 1$.

This says that for any $\varepsilon > 0$, we have $\delta > 0$ s.t. $\phi < \delta \Rightarrow |\frac{f(\phi)}{\gamma_{p,1}(\phi)} - 1| < \varepsilon$.

In particular, for ε^* we have δ^* s.t. for $\phi < \delta^*$

$$\left|\frac{f(\phi)}{\gamma_{p,1}(\phi)} - 1\right| < \varepsilon^* \text{ , so that}$$

$$\frac{f(\phi)}{\gamma_{p,1}(\phi)} - 1 < \varepsilon^* = \exp(\frac{\varepsilon}{r_p(0)}) - 1 \text{ , since by construction } \frac{f(\phi)}{\gamma_{p,1}(\phi)} \geq 1 \ \forall \ \phi,$$

$$\text{which gives } \frac{f(\phi)}{\gamma_{p,1}(\phi)} < \exp\left(\frac{\varepsilon}{r_p(0)}\right) \text{ as needed.}$$

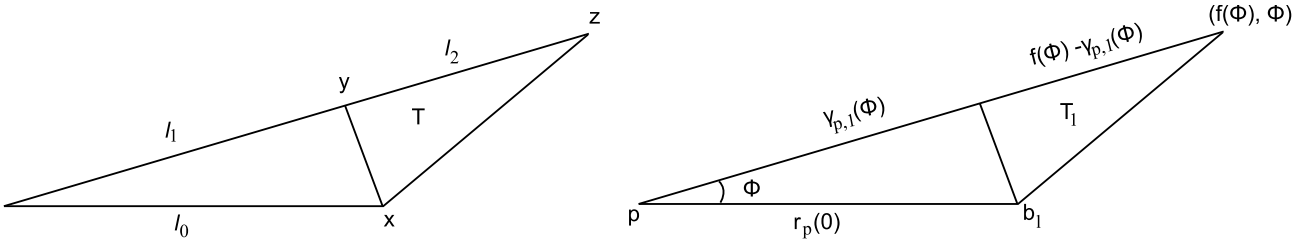

Figure 14: Fithian's Equation: μ(T) = $l_0 \ln(1 + \frac{l_2}{l_1})$

10.4 Falconer's Lemma and Convergence on a Fixed Neighborhood

In [3], Falconer proves a lemma which contains a construction and a map closely related to ours. As such, it contains information useful to us as we seek to prove convergence. He defines a map Ψ which is the inverse of our map σ defined above. Since we use ψ to refer to angles measured from q, we will avoid confusion and call his map σ^{-1}. Note that both σ and σ^{-1} are continuous and 1-1.
Note: If $(x_1, \theta_1) = \sigma(x_0, \theta_0)$, we say $\theta_1 = h(\theta_0)$.

Falconer finds a neighborhood N of b_l with three useful properties:

1. $\sigma^{-1}(N) \subset N$.

2. $\lim_{k\to\infty} \sigma^{-k}(N \cap l_0) \subset N \cap l$, where l_0 is any line intersecting N that is parallel to l. Note that this is a non-trivial limit; namely, it is a line segment in $N \cap l$, rather than a point or $\emptyset$.

We also work to find a neighborhood N' with a third property:

Since $\Omega > 1$, $\exists\ c$ s.t. $\Omega - c > 1$. Recall that in Section 6 we find that $\phi_2 \approx \Omega\phi_1$, where these angles refer to the angles generated by our algorithm. This can equivalently be written $h(\theta) \approx \Omega\theta$.
We use Taylor expansions of $h(\theta)$ about 0 to derive this expression, thus we see that $\lim_{\theta\to 0} \frac{h(\theta)}{\theta} = \Omega$.
This tells us that $\exists\ \delta$ s.t. $\theta < \delta \Rightarrow \frac{h(\theta)}{\theta} > \Omega - c$. Thus if $\lambda := \Omega - c$ and $\theta < \delta$, we get $h(\theta) > \lambda\theta$ and $\lambda > 1$. This is our third property.
We then take our neighborhood $N' := N \cap \{(x, \theta) : 0 < \theta < \delta\}$.

Take a triangle T constructed as above, s.t. $\gamma_{p,1}$ comprises a side of T, $T \subset N'$ and $\mu(T) < \varepsilon$. Clearly

T contains some line segment l_0. Since $N' \subset N$, Property 1. gives us that $\lim_{k\to\infty} \sigma^{-k}(N' \cap l_0) \subset N' \cap l$, a portion of a line, and so we have that $\exists\ m > 0$ s.t. $\sigma^{-(2m-1)}(N')$ does not contain all of T. (We write $(2m-1)$ so as to match notation used in a construction above.) Then consider $T \cap \sigma^{-(2m-1)}(N')$. Since $T \cap \sigma^{-(2m-1)}(N') \subset T$, we get that $\mu(T \cap \sigma^{-(2m-1)}(N')) < \varepsilon$.

Calling on Lemma 10.5, we see that $E_\mu(\gamma_{p,1}) < \varepsilon$ for some range of angles. Then if we take $\sigma^{2m-1}(T \cap \sigma^{-(2m-1)}(N'))$, we only reduce the μ-error (by the same arguments used to show Lemma 10.6), and we land back in N'. Then we end up with an approximation $\gamma_{p,m}$ to $\partial K \cap N'$ s.t. $E_\mu(\gamma_{p,m}) < \varepsilon$ for some range of angles.

Then we have a fixed neighborhood N' s.t. given $\varepsilon > 0$, we can approximate $\partial K \cap N'$ within ε in terms of μ-measure.

(Note: The statement that $h(\theta) > \lambda\theta$ for some $\lambda > 1$ addresses the requirement mentioned in Note 2. following Lemma 10.6. It also lets us deal with the issue presented in Note 1. following the same lemma. In particular, we know the angles we pick are those which hit the vertex of the body contained on the curve inside K, and that this curve lies in N'. Then we know that the upper limit of the range of angles for which our approximation for $\gamma_{p,k}$ is valid does not collapse to 0.)

References

[1] G.L. Butcher, A. Medin, and D.C. Solmon *Planar Convex Bodies with a Common Directed X-Ray*, 2005: Rend. Instit. Mat. Trieste Vol. XXXVII, 1-26

[2] M. Dartmann, *Rekonstrucktion konvexer, homogener Gebiete aus wenigen Punktquellen*, 1991: Diplomarbeit. U. M*ü*nster, Germany

[3] K.J. Falconer *X-Ray Problems for Point Sources*, 1981: Proc. London Math. Soc. (3) 46, 241-262

[4] K.J. Falconer *Hammer's X-Ray Problem and the Stable Manifold Theorem*, 1983: J. London Math. Soc (2), 28, 149-160

[5] D. Fithian, *Verifying A Triangle with Two Directed X-Rays*, 2003: Proceedings of the REU Program in Mathematics, Oregon State University

[6] Richard J. Garnder *Symmetrals and X-Rays of Planar Convex Bodies*, 1983: Arch. Math. 4, 183-189

[7] Richard J. Gardner *Geometric Tomography: Second Edition*, 1995: Cambridge Press

[8] Jason Siekfen and Lena Spargo *An Algorithm for Reconstruction of a Convex Body from Two Point Sources*, 2005: Proceedings of the REU Program in Mathematics, Oregon State University